Bound Photon Orbits in Kerr de Sitter spacce times.

Eunice Omwoyo,Humberto Belich,Júlio C. Fabris,Hermano Velten

Universidade Federal do Espírito Santo

Agenda

General Information

- The Event Horizon Telescope has shown the images at the centre of M87* and Sagittarius A (Sgr A).

Figura 1: M87.

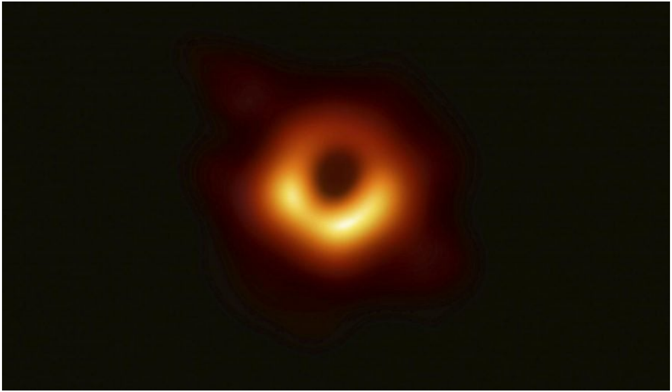

Figura 2: Sagittarius A.

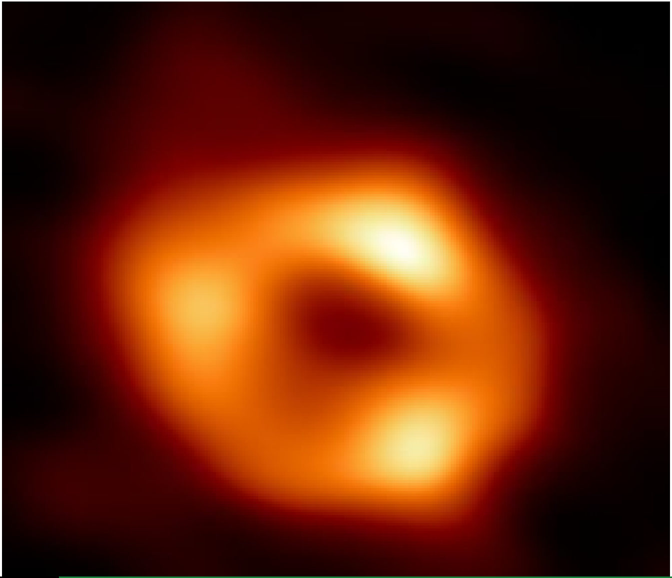

What does the future hold?

At high resolution

Figura 3: GRMHD simulation of a black hole shadow. The very sharp razor thin ring of light ("Photon Ring.")

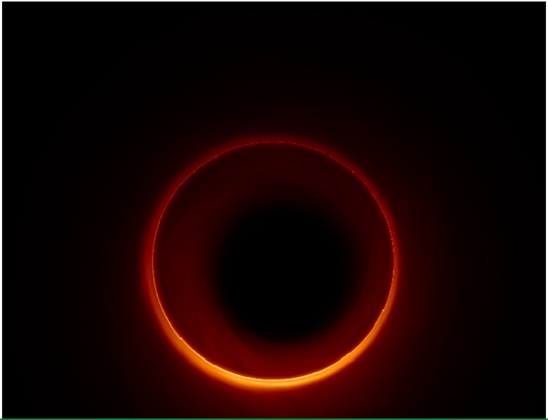

What is the origin of the Photon Ring

Structure of the Photon Ring

- The photon ring is composed of self similar subrings indexed by the number of photon orbits around the black hole.
- These subrings are entirely governed by three critical parameters δ, γ and ζ.
- The photon ring is not only visible in the image but also in VLBI. The signatures can be detected by future detectors.

Figura 4

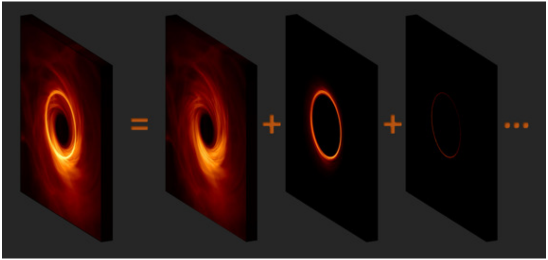

Why do we care about the photon ring?

- Since the photon ring is matter independent, measuring it can then provide a test of general relativity and gravity in the strong field regime.

How can we understand the photon ring

- To understand the photon ring, knowledge of bound photon orbits is crucial.

Our work

- The main objective of this work is analysis of bound photon orbits in KdS and RKdS space time.
- From which we then obtain the critical parameters that govern the structure of the sub rings in these space times.
- We analyze the orbits that asymptote the bound photon orbits.
- We generalize our analysis to a Schwarzchild black hole.

KdS

The null geodesic equations in KdS space time are given as,

$$\frac{\Sigma}{E}p^r = \pm_r\sqrt{R(r)}, \frac{\Sigma}{E}p^\theta = \pm_\theta\sqrt{\Theta(\theta)}, \tag{1}$$

$$\frac{\Sigma}{E}p^\phi = \frac{aL^2}{\Delta_r}(a(a-\lambda)+r^2) - \frac{L^2}{\Delta_\theta \sin^2\theta}(a\sin^2\theta - \lambda), \tag{2}$$

$$\frac{\Sigma}{E}p^t = \frac{L^2}{\Delta_r}((r^2+a^2)^2 - a\lambda(a^2+r^2)) - \frac{aL^2}{\Delta_\theta}(a\sin^2\theta - \lambda). \tag{3}$$

Where,

$$R(r) = L^2(r^2+a^2-a\lambda)^2 - \Delta_r(\eta + L^2(\lambda - a)^2), \tag{4}$$

$$\Theta(\theta) = a^2\Delta_\theta L^2 + a^2L^2\cos^2(\theta) - a^2L^2 - 2a\Delta_\theta\lambda L^2 + 2a\lambda L^2 + \Delta_\theta\eta + \Delta_\theta\lambda^2L^2 - \lambda^2L^2\cot \tag{5}$$

KdS

We first reparametrize the equations by the "Mino time"τ parameter

$$\frac{\Sigma}{E} p^{\mu} = \frac{dx^{\mu}}{d\tau} \tag{6}$$

Secondly, We convert them into integral forms as,

$$I_{\theta} = \int_{\theta_s}^{\theta_o} \frac{d\theta}{\pm\sqrt{\Theta(\theta)}}, \tag{7}$$

$$I_r = \int_{r_s}^{r_o} \frac{dr}{\pm\sqrt{R(r)}}, \phi_o - \phi_s = \frac{\left(aL^2\right)\left(a(a-\lambda)+\mathrm{r}^2\right)}{\Delta_r} I_r - L^2 a I_{\phi} + L^2 \lambda \bar{I}_{\phi}, \tag{8}$$

$$t_o - t_s = \frac{L^2}{\Delta_r}((r^2+a^2)^2 - a\lambda(a^2+r^2))I_r + a^2 L^2 I_t - aL^2(a-\lambda) I_{\phi}, \tag{9}$$

Where we have defined,

$$I_{\phi} = \int_{\theta_s}^{\theta_o} \frac{d\theta}{\pm_r \sqrt{\Theta(\theta)}\Delta_{\theta}}, \bar{I}_{\phi} = \int_{\theta_s}^{\theta_o} \frac{d\theta}{\pm_{\theta}\sqrt{\Theta(\theta)}\Delta_{\theta}\sin^2\theta}, I_t = \int_{\theta_s}^{\theta_o} \frac{\cos^2\theta d\theta}{\pm_{\theta}\sqrt{\Theta(\theta)}\Delta_{\theta}}. \tag{10}$$

Solutions

After some long calculations we obtain

Latitudinal Motion Trajectory

$$\theta_o(\tau) = \arccos\left(-\sqrt{u_+}\nu_\theta sn\left[\left(\tau\sqrt{-u_-\Xi} - \nu_\theta F\left(\varphi_s|k\right)\right) \mid k\right]\right) \tag{11}$$

u_+ and u_- are related to the roots of the angular potential

Azimuthal Motion Trajectory

$$\phi_o - \phi_s = \frac{\left(aL^2\right)\left(a(a-\lambda)+\mathrm{r}^2\right)}{\Delta_r}\tau - L^2 aI_\phi + L^2\lambda\bar{I}_\phi \tag{12}$$

Temporal Motion Trajectory

$$t_o - t_s = \frac{L^2}{\Delta_r}((r^2+a^2)^2 - a\lambda(a^2+r^2))\tau + a^2L^2I_t - aL^2(a-\lambda)I_\phi \tag{13}$$

Where,

$$I_\phi = \frac{1}{\sqrt{-u_-\Xi}}\left[\nu_\theta \Pi(-yu_+, \varphi_s, k) - \nu_\theta \Pi(-yu_+, \varphi_\tau, k)\right], \tag{14}$$

$$\begin{aligned}\bar{I}_\phi = \frac{1}{\sqrt{-u_-\Xi}}\frac{1}{1+y}\left[\nu_\theta(\Pi(u_+, \varphi_s, k) + y\Pi(-yu_+, \varphi_s, k))\right] - \\ \frac{1}{\sqrt{-u_-\Xi}}\frac{1}{1+y}\left[\nu_\theta(\Pi(u_+, \varphi_\tau \mid k) + y\Pi(-yu_+, \varphi_\tau \mid k))\right],\end{aligned} \tag{15}$$

$$I_t = \frac{u_+}{\sqrt{-u_- \Xi}} \left[\nu_\theta J(-yu_+, \varphi_s \mid k) - \nu_\theta J(-yu_+, \varphi_\tau \mid k) \right] \tag{16}$$

$$\Delta_r = \left(1 - \frac{\Lambda r^2}{3}\right)(r^2 + a^2) - 2Mr \tag{17}$$

The parameters $F(x \mid k)$ and $\Pi(n, x \mid k)$ are the Elliptic integrals of first and third kind respectively. Moreover, $J(n, x \mid k)$ is related to the Carlson's integral, R_j, through the relation,

$$J(n, x \mid k) = \frac{1}{3} \sin^3(x) R_J \left(\cos^2(x), 1 - k \sin^2(x), 1, 1 - n \sin^2(x) \right) \tag{18}$$

Examples of selected orbits.

Figura 5: Zero Angular Momentum Orbit, $\lambda = 0$. The pink arrow shows the poles. $\theta_1 = 0$, $\theta_4 = \pi$

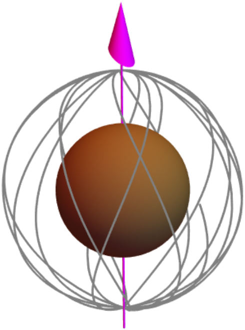

Figura 6: Orbit at $r = 1.76M$, $\theta_1 = 0.737886$ and $\theta_2 = 2.40371$

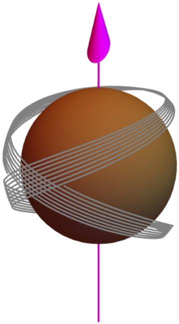

Figura 7: Equatorial circular prograde orbit, $\theta_1 = \pi/2$ and $\theta_2 = \pi/2$

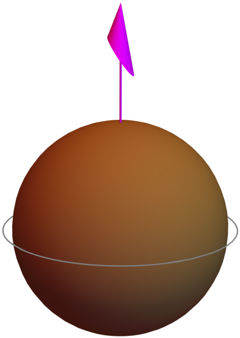

Figura 8: Equatorial circular retrograde orbit, $\theta_1 = \pi/2$ and $\theta_2 = \pi/2$

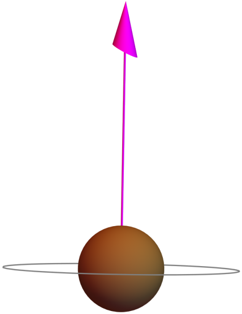

These orbits experience different time delays (the amount of time they take to complete half orbits), Lyapunov exponents (the rate of exponential deviation of nearby orbits) and change in azimuthal angle. We derive the equations for these three parameters.

Critical Parameters

Change in azimuthal angle,δ

$$\delta = 2\left(\frac{(aL^2)\left(a(a-\lambda)+\mathrm{r}^2\right)}{\Delta_r}\Gamma_\theta - L^2 a\Gamma_\phi + L^2\lambda\bar{\Gamma}_\phi\right), \tag{19}$$

This gives how much the azimuthal angle changes for half an orbit.

Time delay

$$\zeta = 2\left(\frac{L^2}{\Delta_r}((r^2+a^2)^2 - a\lambda(a^2+r^2))\Gamma_\theta + a^2L^2\Gamma_t - aL^2(a-\lambda)\Gamma_\phi\right). \tag{20}$$

Time delay gives how much t changes for half an orbit.

Lyapunov Exponent

$$\gamma = \sqrt{\frac{1}{3}\Lambda\left(a^2+6r^2\right)\left(L^2(a-\lambda)^2+\eta\right)+L^2\left(a^2-\lambda^2+6r^2\right)-\eta\Gamma_\theta} \tag{21}$$

The Lyapunov exponent demonstrates how quickly nearby geodesics will deviate exponentially.

Analysis of the critical Parameters

Figura 9: Modelling the time delay of KdS black hole to Sgr A, with $M = 4 \times 10^6 M_\odot$ and $\theta = 30^\circ$

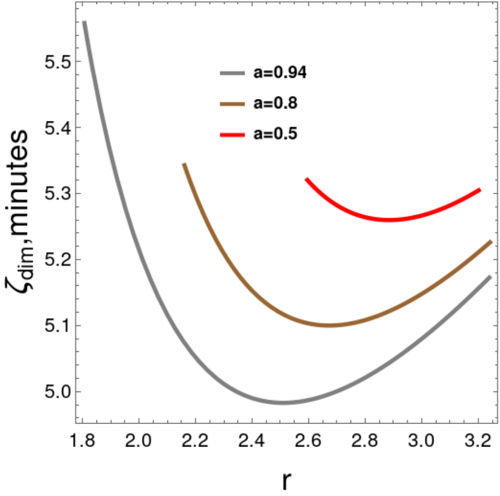

Figura 10: Modelling the time delay of KdS black hole to Sgr A, with $M = 6 \times 10^9 M_\odot$ and $\theta = 30^\circ$

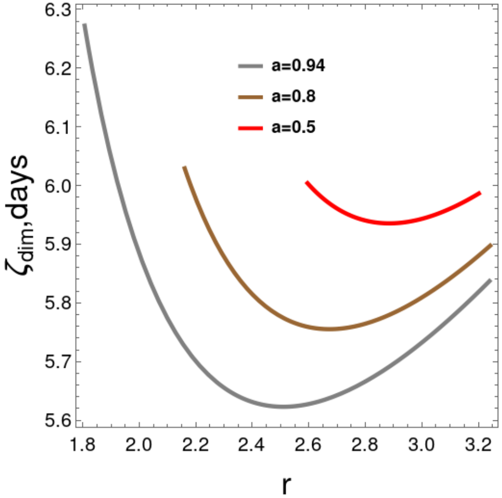

Sgr A

In Sgr A, when $a = 0.94, 0.8, 0.5$, the time delay ranges within $\zeta_{dim} \in [4.98352, 5.5589], [5.10068, 5.34345], [5.26041, 5.32105]$ minutes respectively.

M87

In Sgr A, when $a = 0.94, 0.8, 0.5$, the time delay ranges within $\zeta_{dim} = [5.62376, 6.27306], [5.75597, 6.02994], [5.93623, 6.00465]$ days respectively.

In the case of a rapidly rotating black hole, such as $a = 0.99999$ with an observer inclined on the equatorial plane, the time delay range for SgrA ranges within $\zeta_{dim} = [4.92024, 463.102]$ minutes, whereas M87 will be $\zeta_{dim} = [5.55235, 522.598]$ days.

Change in Azimuthal Angle Parameter

Figura 11: Change in azimuthal angle in a KdS black hole. The observer inclination is 30°.The change in azimuthal angle parameter decreases monotonically from $r_{ph+,KdS}$ to $r_{ph-,KdS}$.

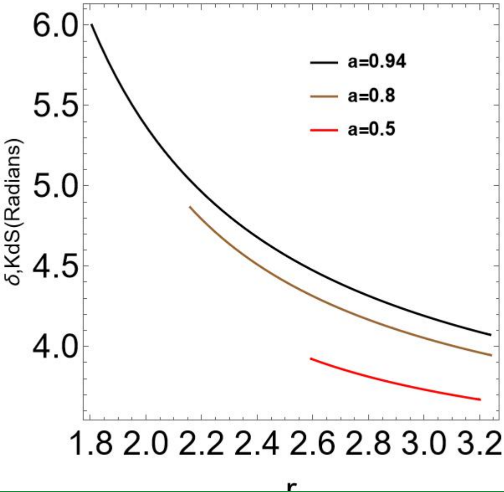

Figura 12: Change in azimuthal angle in a KdS black hole. The observer inclination is 30°.The change in azimuthal angle parameter decreases monotonically from $r_{ph+,KdS}$ to $r_{ph-,KdS}$. Change in azimuthal angle is indistinguishable for $\Lambda = 0$ and $\Lambda = 1.11 \times 10^{-52}$

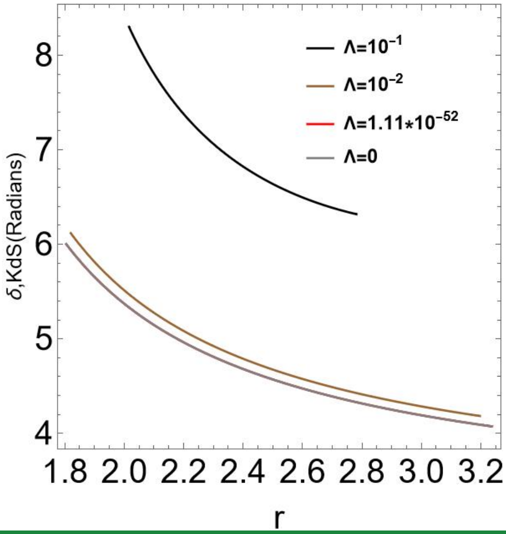

Lyapunov Exponent

Before analysing the Lyapunov exponent, discuss a little about nearly bound photon orbits

Radial Motion

$$r_o^E[\tau] = \frac{r_3(r_1 - r_3)\mathrm{sn}^2\left(\frac{\tau}{g_E} + \nu_r F(\varphi_{E,s}|k_E)\middle| k_E\right) + r_3(r_3 - r_1)}{(r_1 - r_3)\mathrm{sn}^2\left(\frac{\tau}{g_E} + \nu_r F(\varphi_{E,s}|k_E)\middle| k_E\right) - r_1 + r_3} \tag{22}$$

Azimuthal Motion

$$\phi_o - \phi_s = \frac{-aL^2 3}{\Lambda}\left(\frac{\left(a^2 - a\lambda + r_c^2\right) I_c}{(r_c - r_{--})(r_c - r_{h-})(r_c - r_{h+})} - \frac{\left(a^2 - a\lambda + r_{--}^2\right) I_{--}}{(r_c - r_{--})(r_{--} - r_{h-})(r_{--} - r_{h}}\right.$$
$$\left. + \frac{aL^2 3}{\Lambda}\left(\frac{\left(a^2 + {r_{h-}}^2 - a\lambda\right) I_{h-}}{(r_c - r_{h-})(-r_{--} + r_{h-})(r_{h-} - r_{h+})} + \frac{\left(a^2 + {r_{h+}}^2 - a\lambda\right) I_{h+}}{(r_c - r_{h+})(-r_{--} + r_{h+})(-r_{h-} + r_{h+})}\right)\right.$$
$$- L^2 a I_\phi + L^2 \lambda \bar{I}_\phi, \tag{23}$$

Temporal Motion

$$t_o - t_s = \frac{3L^2\left(a^2+r_{--}^2\right)\left(a^2-a\lambda+r_{--}^2\right)I_{--}}{\Lambda(r_c-r_{--})(r_{--}-r_{h-})(r_{--}-r_{h+})} + \frac{3L^2\left(a^2+r_{h-}^2\right)\left(a^2-a\lambda+r_{h-}^2\right)I_{h-}}{\Lambda(r_c-r_{h-})(r_{h-}-r_{--})(r_{h-}-r_{h+})}$$
$$+\frac{3L^2\left(a^2+r_{h+}^2\right)\left(a^2-a\lambda+r_{h+}^2\right)I_{h+}}{\Lambda(r_c-r_{h+})(r_{h+}-r_{--})(r_{h+}-r_{h-})} - \frac{3L^2\left(a^2+r_c^2\right)\left(a^2-a\lambda+r_c^2\right)I_c}{\Lambda(r_c-r_{--})(r_c-r_{h-})(r_c-r_{h+})} - \frac{3L^2 I_r}{\Lambda}$$
$$+ a^2L^2I_t - aL^2(a-\lambda)I_\phi. \quad (24)$$

Where,

$$I_x = -\frac{2(r_4-r_3)(\Pi_o-\Pi_s)}{(r_x-r_4)(r_x-r_3)\sqrt{(r_4-r_2)(r_3-r_1)}} - \frac{2(F_o-F_s)}{(r_x-r_3).\sqrt{(r_4-r_2)(r_3-r_1)}} \quad (25)$$

$$\Pi_{s,o} = \Pi\left(\frac{(r_4-r_1)(r_x-r_3)}{(r_x-r_4)(r_3-r_1)};\varphi_{E,s,o}|k\right), F_{s,o} = F\left(\varphi_{E,s,o}|k\right) \quad (26)$$

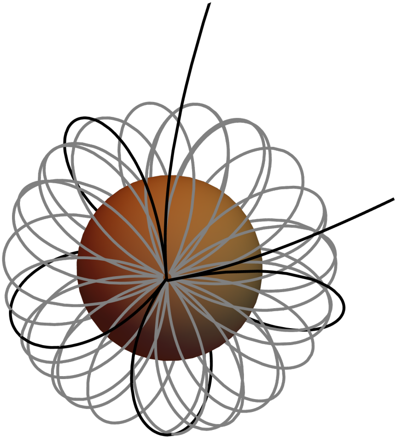

Figura 13: A nearly bound orbit asymptoting the zero angular momentum orbit before escaping

Figura 14: A nearly bound orbit asymptoting a bound photon orbit at $r = 3.56M$ before escaping

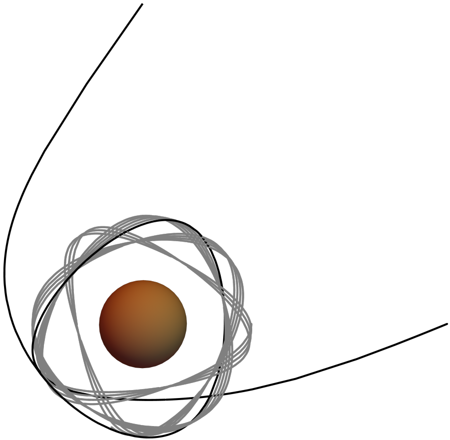

Figura 15: A nearly bound orbit asymptoting the equatorial circular prograde orbit before escaping

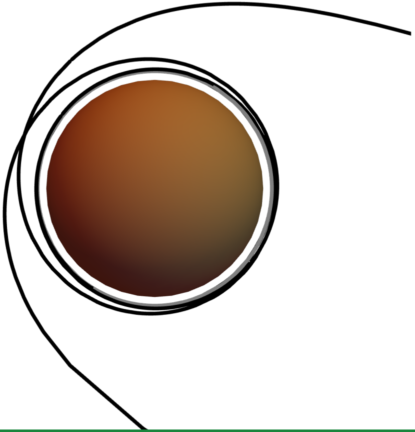

Figura 16: A nearly bound orbit asymptoting the zero angular momentum orbit before plunging into the black hole.

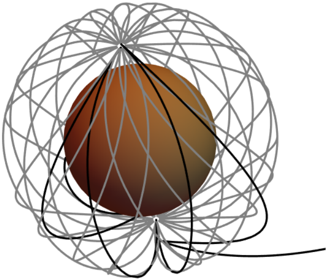

Figura 17: A nearly bound orbit asymptoting a bound photon orbit at $r = 3.56M$ before plunging into the black hole.

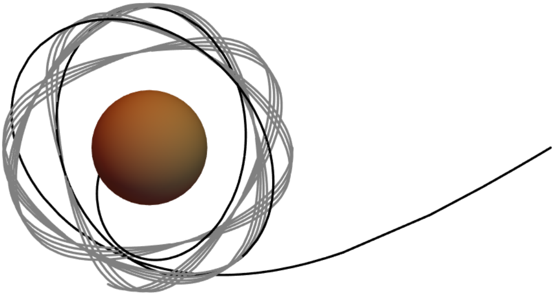

Figura 18: A nearly bound orbit asymptoting the equatorial circular prograde orbit before plunging into the black hole.

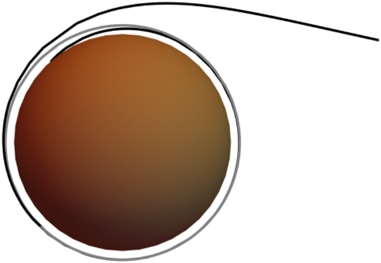

The rate at which the distance between these orbits grows is governed by the Lyapunov exponent. This exponent in turn governs the thickness of the subrings in the shadow.

Figura 19: Lyapunov exponent for observers inclined at 30°.

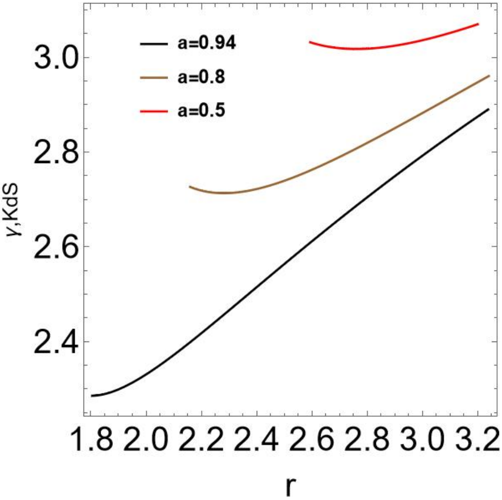

Figura 20: Lyapunov exponent for observers inclined at 90°.

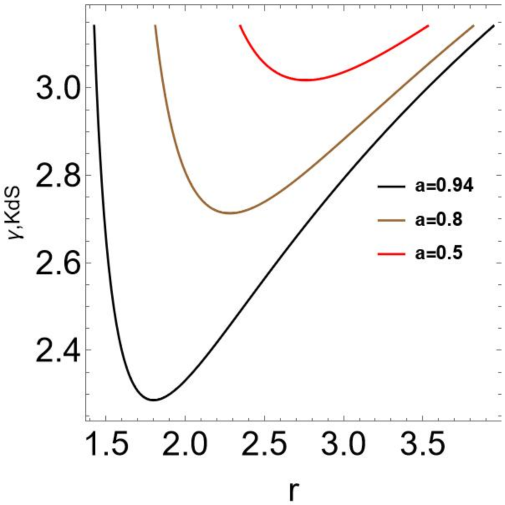

Figura 21: Lyapunov exponent for observers inclined at 30°.

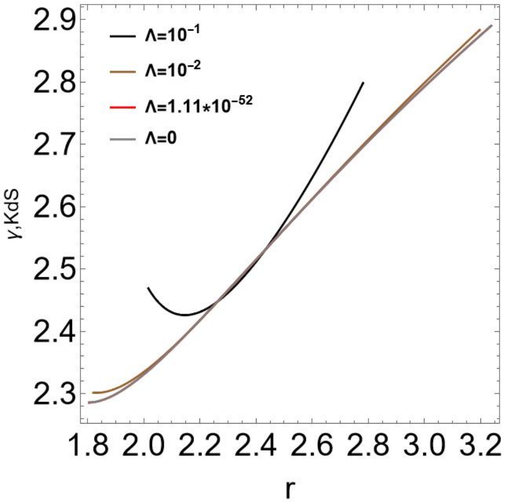

Kerr de Sitter Revisited

Polar Motion

$$\theta_o = \arccos\left(-\sqrt{\hat{u}_+}\nu_\theta sn\left[\tau\sqrt{-\hat{u}_- a^2} - \nu_\theta F(\hat{\psi}_s \mid \hat{k}) \mid \hat{k}\right]\right). \tag{27}$$

Azimuthal Motion

$$\hat{\phi}_o - \hat{\phi}_s = \left(\frac{ar^2 + a^3 - a\hat{\Delta} - a^2\hat{\lambda}}{\hat{\Delta}}\right)\tau + \hat{\lambda}\hat{I}_\phi, \tag{28}$$

Temporal Motion

$$t_o - t_s = \left(\frac{(r^2 + a^2)(r^2 + a^2 - a\lambda)}{\hat{\Delta}} + a\hat{\lambda} - a^2\right)\tau + a^2\hat{I}_t. \tag{29}$$

$$\hat{I}_\phi = \frac{1}{\sqrt{-u_- a^2}} \left(\nu_\theta \Pi(\hat{u}_+; \hat{\psi}_s \mid \hat{k}) - \nu_\theta \Pi(\hat{u}_+; \hat{\psi}_\tau \mid \hat{k}) \right) \tag{30}$$

$$\hat{I}_t = \frac{\hat{u}_+}{\hat{k}\sqrt{-u_- a^2}} \left(\nu_\theta [F(\hat{\psi}_s \mid \hat{k}) - E(\hat{\psi}_s \mid \hat{k})] - \nu_\theta [F(\hat{\psi}_\tau \mid \hat{k}) - E(\hat{\psi}_\tau \mid \hat{k})] \right), \tag{31}$$

Figura 22: A zero angular momentum orbit around a RKdS black hole.

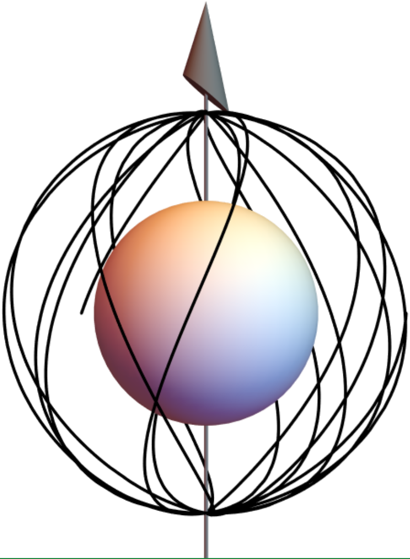

Figura 23: A bound orbit at $r = 1.76M$ around a RKdS black hole.

Critical Parameters

Change in azimuthal angle parameter

$$\hat{\delta} = \left(\frac{ar^2 + a^3 - a\hat{\Delta} - a^2\hat{\lambda}}{\hat{\Delta}}\right)\left(\frac{2}{\sqrt{-\hat{u}_- a^2}}K(\hat{k})\right) + \hat{\lambda}\left(\frac{2}{\sqrt{-u_- a^2}}\Pi(\hat{u}_+ \mid \hat{k})\right), \quad (32)$$

Time Delay

$$\hat{\zeta} = \left(\frac{(r^2 + a^2)(r^2 + a^2 - a\lambda)}{\hat{\Delta}} + a\hat{\lambda} - a^2\right)\left(\frac{2}{\sqrt{-\hat{u}_- a^2}}K(\hat{k})\right) + a^2\left(\frac{2\hat{u}_+}{\hat{k}\sqrt{-u_- a^2}}[K(\hat{k}) - E(\hat{k})]\right) \quad (33)$$

Lyapunov Exponent

$$\hat{\gamma} = (\frac{2}{\sqrt{-\hat{u}_{-}a^{2}}}K(\hat{k}))\sqrt{\frac{1}{3}\Lambda\left(a^{2}+6r^{2}\right)\left(L^{2}(a-\hat{\lambda})^{2}+\hat{\eta}\right)+L^{2}\left(a^{2}-\hat{\lambda}^{2}+6r^{2}\right)-\hat{\eta}}. \tag{34}$$

Time Delay

Figura 24: Modeling the time delay in RKdS to M87 black hole

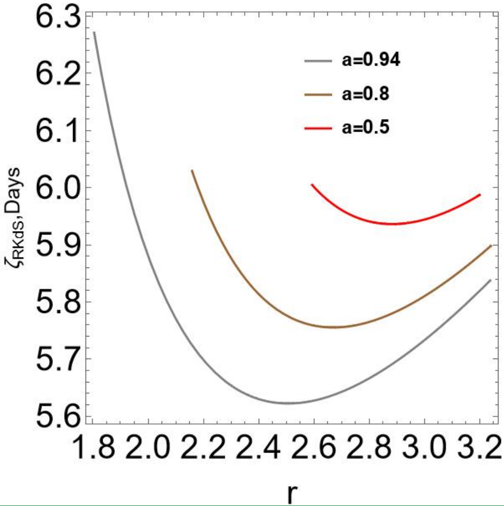

Figura 25: Modeling the time delay in RKdS to SgrA black hole

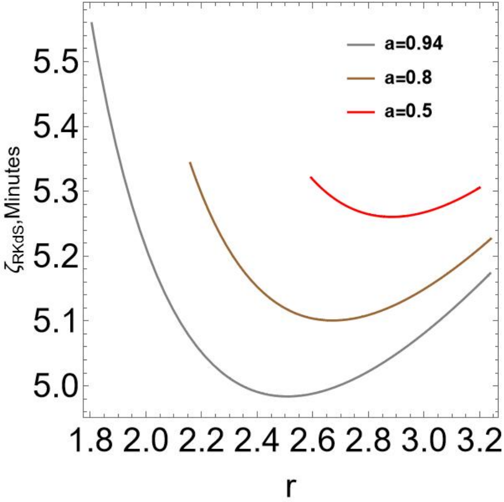

Change in Azimuthal angle

Figura 26: Change in azimuthal angle in RKdS black hole for observers inclined at 30°

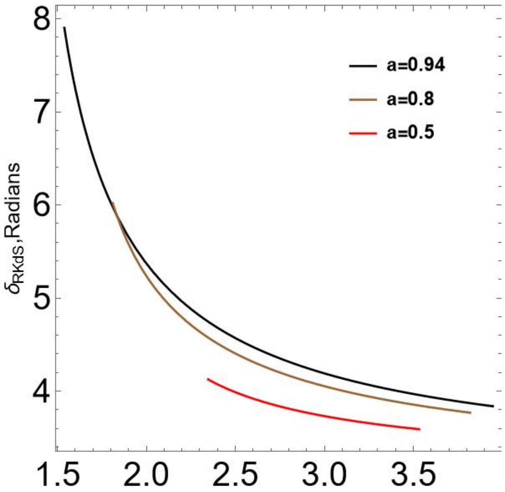

Figura 27: Change in azimuthal angle in RKdS black hole for observers inclined at 30°

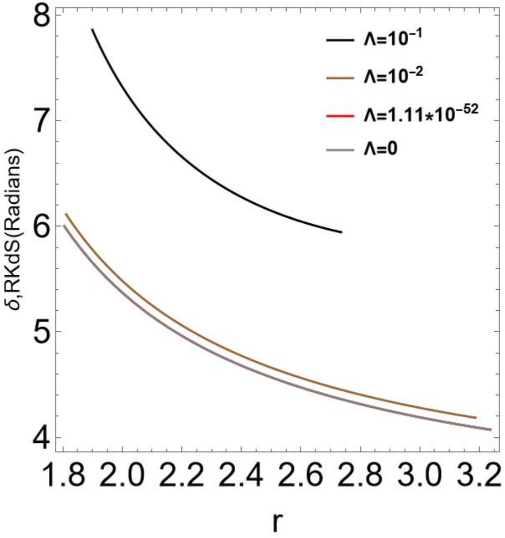

Lyapunov Exponent

Nearly Bound photon orbits in RKdS

We have obtained the solutions for these orbits. At the moment, we are testing their results in the code.

Figura 28: A nearly bound orbit around a RKdS black hole asymptoting the zero angular momentum orbit before escaping

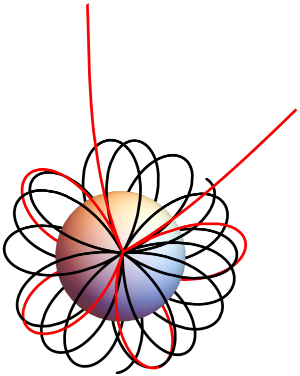

Figura 29: A nearly bound orbit around a RKdS black hole asymptoting a bound photon orbit at $r = 3.56M$ before escaping

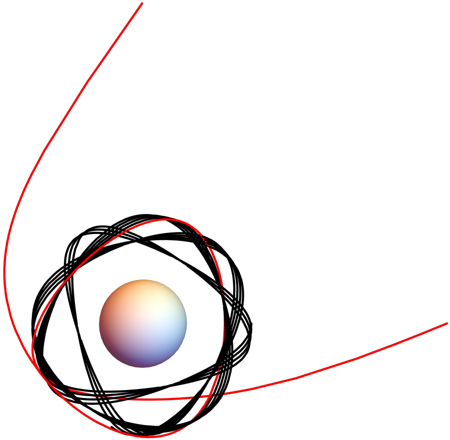

The Lyapunov exponent gives the rate of exponential deviation of the distance between these orbits. This exponent in turn controls the thickness of the subsequent photon rings.

Figura 30: Lyapunov exponent for observers inclined at 30°

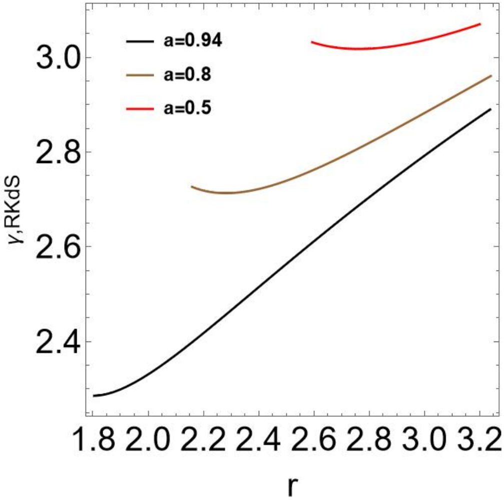

Figura 31: Lyapunov exponent for observers inclined at 30°

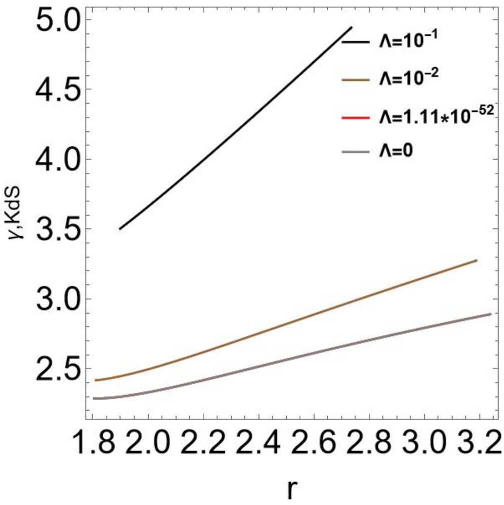

Is time delay related to any aspect of the photon ring?

Figura 32: Time delay

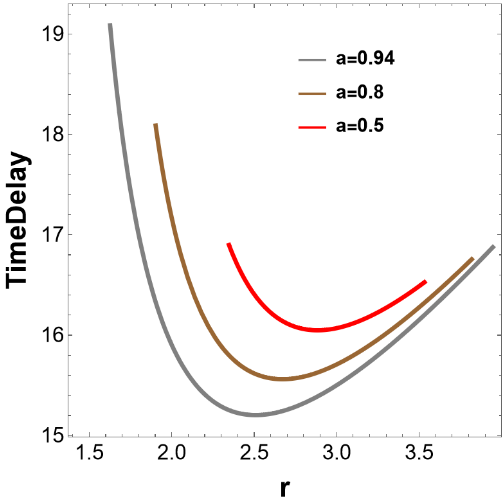

Figura 33: Time delay

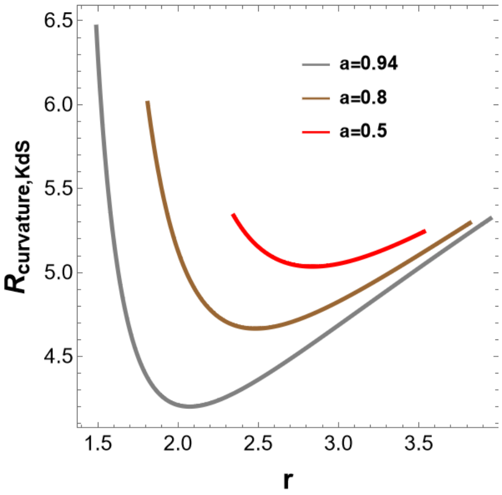

Tabela 1: Time Delay Parameter with $\theta = 30^\circ$, $a = 0.9$ for different values of Λ. Note that for the column of a Kerr black hole,$\Lambda = 0$.

Λ	r/M	Kerr	kds	rkds
$1.11 \times 10^{-52} m^2$	2.6	15.3167	15.3167	15.3167
	2.5	15.3204	15.3204	15.3204
	2.2	15.6165	15.6165	15.6165
$10^{-30} m^2$	2.6	15.3167	15.3167	15.3167
	2.5	15.3204	15.3204	15.3204
	2.2	15.6165	15.6165	15.6165
$10^{-10} m^2$	2.6	15.3167	15.3167	15.3167
	2.5	15.3204	15.3204	15.3204
	2.2	15.6165	15.6165	15.6165
$10^{-5} m^2$	2.6	15.3167	15.3173	15.3172
	2.5	15.3204	15.321	15.3209
	2.2	15.6165	15.6171	15.617
$10^{-2} m^2$	2.6	15.3167	15.9408	15.8412
	2.5	15.3204	15.9412	15.8387
	2.2	15.6165	16.2587	16.138
$10^{-1} m^2$	2.6	15.3167	29.6076	25.5734
	2.5	15.3204	29.4009	25.3434
	2.2	15.6165	30.55	25.6301

Tabela 2: Change in azimuthal angle Parameter with $\theta = 30^{\circ}$, $a = 0.9$ for different values of Λ. Note that for the column of a Kerr black hole, $\Lambda = 0$.

Λ	r/M	Kerr	kds	rkds
$1.11 \times 10^{-52} m^2$	2.6	4.42902	4.42902	4.42902
	2.5	4.52374	4.52374	4.52374
	2.2	4.9161	4.9161	4.9161
$10^{-30} m^2$	2.6	4.42902	4.42902	4.42902
	2.5	4.52374	4.52374	4.52374
	2.2	4.9161	4.9161	4.9161
$10^{-10} m^2$	2.6	4.42902	4.42902	4.42902
	2.5	4.52374	4.52374	4.52374
	2.2	4.9161	4.9161	4.9161
$10^{-5} m^2$	2.6	4.42902	4.42911	4.4291
	2.5	4.52374	4.52384	4.52383
	2.2	4.9161	4.91621	4.91621
$10^{-2} m^2$	2.6	4.42902	4.52784	4.51767
	2.5	4.52374	4.62599	4.61381
	2.2	4.9161	5.03575	5.01565
$10^{-1} m^2$	2.6	4.42902	6.47098	6.02759
	2.5	4.52374	6.62686	6.13723
	2.2	4.9161	7.47017	6.70676

Tabela 3: Lyapunov exponent with $\theta = 30^\circ$, $a = 0.9$ for different values of Λ. Note that for the column of a Kerr black hole,$\Lambda = 0$.

Λ	r/M	Kerr	kds	rkds
$1.11 \times 10^{-52} m^2$	2.6	2.65606	2.65606	2.65606
	2.5	2.61516	2.61516	2.61516
	2.2	2.50465	2.50465	2.50465
$10^{-30} m^2$	2.6	2.65606	2.65606	2.65606
	2.5	2.61516	2.61516	2.61516
	2.2	2.50465	2.50465	2.50465
$10^{-10} m^2$	2.6	2.65606	2.65606	2.65606
	2.5	2.61516	2.61516	2.61516
	2.2	2.50465	2.50465	2.50465
$10^{-5} m^2$	2.6	2.65606	2.65606	2.65609
	2.5	2.61516	2.61516	2.61519
	2.2	2.50465	2.50465	2.50467
$10^{-2} m^2$	2.6	2.65606	2.47334	2.68412
	2.5	2.61516	2.61489	2.64209
	2.2	2.50465	2.50587	2.52933
$10^{-1} m^2$	2.6	2.65606	2.67491	2.84961
	2.5	2.61516	2.61565	2.78954
	2.2	2.50465	2.55747	2.6735

We also generalize our calculations to Schwarzschild de Sitter space time.

- Derived the bound geodesics.
- Derived the critical parameters.
- Analyze the critical parameters.
- Code to plot the geodesics.

Conclusion

- We have analyzed the bound photon orbits in KdS and RKdS space time.
- We have analyzed the critical parameters that control the structure of the photon rings.
- We observe that there could be a direct relationship between the time delay parameter and radius of curvature of the critical curve.
- Moreover, we have analyzed the nearly bound photon orbits.
- For the astrophysically relevant value of the cosmological constant, the structure of the photon rings in KdS, RKdS and Kerr black hole are indistinguishable.


OBRIGADA